COMMUNICATIONS IN SCIENCE AND TECHNOLOGY
Homepage: cst.kipmi.or.id

Dual metal NiMo dispersed on silica derived from rice husk ash as a catalyst for hydrocracking of used palm cooking oil into liquid biofuels

Karna Wijaya[a], Risandrika Dwijayanti Putri Setyono[a], Remi Ayu Pratika[b], Eddy Heraldy[c], Ahmad Suseno[d], Lukman Hakim[e], Iqmal Tahir[a], Won-Chun Oh[f], Aldino Javier Saviola[a,*]

[a]*Department of Chemistry, Universitas Gadjah Mada, Yogyakarta 55281, Indonesia*
[b]*Study Program of Chemistry, Universitas Palangka Raya, Palangka Raya 73111, Indonesia*
[c]*Department of Chemistry, Universitas Sebelas Maret, Surakarta 57126, Indonesia*
[d]*Department of Chemistry, Universitas Diponegoro, Semarang 50275, Indonesia*
[e]*Department of Chemistry, Universitas Brawijaya, Malang 65145, Indonesia*
[f]*Department of Advanced Materials and Engineering, Hanseo University, Chungnam 356-706, Republic of Korea*

Article history:
Received: 11 July 2024 / Received in revised form: 7 September 2024 / Accepted: 7 October 2024

Abstract

The production of vegetable-based fuels has intensified in recent years due to the decreasing availability of fossil fuels and their environmental impacts. This study explores the synthesis, characterization, and application of nickel-molybdenum (NiMo) bimetal-dispersed silica catalysts for converting used palm cooking oil into liquid biofuels. The catalysts were synthesized using the wet impregnation method, incorporating Ni and Mo metals at concentrations of 1, 2, and 3% by weight of silica derived from rice husk ash. Impregnation of the silica with Ni and Mo metals increased its acidity, with the NiMo/SiO_2 2 catalyst exhibiting the highest acidity value of 4.34 mmol/g. This catalyst also demonstrated the largest specific surface area and total pore volume, measured at 205.51 m^2/g and 0.88 cm^3/g, respectively. Hydrocracking of used palm cooking oil into liquid biofuels was performed at an optimum temperature of 450 °C with catalyst-to-feed weight ratios of 1:100, 2:100, and 3:100 for 1 h by hydrogen gas supply of 20 mL/min. Catalyst activity tests revealed the highest mass percentage of liquid product, 23.3%, at a ratio of 1:100 (w/w), with a biofuel yield of 20.34%, comprising 14.20% gasoline and 6.14% diesel. By utilizing biomass waste as both a catalyst and feedstock, this study presents a sustainable approach to reducing the carbon footprint and promoting environmental balance.

Keywords: Silica catalyst; nickel-molybdenum impregnation; biofuel; used palm cooking oil; hydrocracking.

1. Introduction

Petroleum-derived fuels are generally considered expensive. The increasing reliance on fuel consumption has raised concerns about potential depletion of supplies over time, leading to sustained price escalations. Fossil fuel oil (FFO), sourced from non-renewable fossil reserves, represents a finite energy resource that diminishes as consumption rises [1,2]. To address the anticipated scarcity of fossil fuels and transition towards renewable energy sources, various efforts are being implemented. The government has established a proactive target to increase the contribution of renewable energy to approximately 20% by 2025 while reducing reliance on petroleum as an energy source from 52% to 20% [3]. One promising solution for achieving renewable energy diversification is the development of vegetable-based fuels, commonly referred to as biofuels [4].

Vegetable-based fuel (VBF) serves as a viable alternative to fossil-based fuels. Compared to conventional petroleum-based fuels, VBFs are more economical and environmentally sustainable [5]. Frequently termed "green energy", these fuels are derived from eco-friendly sources and exhibit lower greenhouse gas emissions, representing a sustainable alternative [6]. Indonesia, as an agrarian nation, possesses considerable potential for developing the vegetable-based fuel industry, supported by the abundant availability of energy crop raw materials across its regions [7]. Despite this potential, the contribution of vegetable-based fuels to Indonesia's national energy mix remains relatively limited, accounting for only 5% of total renewable energy consumption as of 2025 [8]. The country has developed several types of vegetable-based fuels, including biodiesel, bioethanol, bio-jet fuel, and biogasoline. These biofuels are typically produced from renewable plant-based raw materials such as palm oil, palm kernel oil, coconut oil, jatropha oil, castor oil, and *Calophyllum inophyllum* oil [9–12].

Palm oil is one of the key feedstocks for biofuel production due to its high long-chain hydrocarbon content, low cost, and high biofuel yield [11]. Used palm cooking oil, a by-product of

* Corresponding author. Tel.: +6289503170665
Email: aldino.javier@mail.ugm.ac.id
https://doi.org/10.21924/cst.9.2.2024.1480

palm oil or cooking oil, presents a valuable raw material for biofuel production. This approach not only reduces oil waste but also generates an alternative fuel that is both economically beneficial and environmentally friendly [12–14]. Additionally, used palm cooking oil retains significant fatty acid content, making it a suitable feedstock for biofuel production. The conversion of used palm cooking oil into biofuel is typically achieved through catalytic hydrocracking—a hydrogenation process requiring a catalyst to facilitate hydrogen binding [8,15].

The selection of an appropriate catalyst is critical to achieving optimal results in the hydrocracking process. Numerous studies have explored the use of heterogeneous catalysts for converting used palm cooking oil into biofuels. These catalysts are advantageous due to their thermal stability, ease of recycling, and separation properties [10,15]. In this study, silica (SiO_2) derived from rice husk ash is employed as a catalyst support material. Rice husk ash is abundant, cost-effective, and contains approximately 95% silica by dry weight following combustion [16]. This agricultural by-product, often discarded as waste, contributes to environmental damage and water pollution [17]. Utilizing rice husk ash as a silica source not only mitigates waste-related issues but also offers an environmentally sustainable solution, encouraging more sustainable practices.

Silica-based catalysts exhibit high activity, selectivity, and thermal stability [18]. As demonstrated by Alisha et al. [19], silica extracted from beach sand has shown promising results in converting used palm cooking oil into biofuels, yielding liquid products at 38.38% and 31.92%, respectively. To enhance these functions, catalyst synthesis modifications, such as metal impregnation, are necessary. Metal impregnation optimizes the acidic properties of silica, improving its performance as a heterogeneous catalyst [15]. According to Trisunaryanti et al. [20], catalyst acidity can be increased by incorporating transition metals with empty 4p orbitals, which function as Lewis acid sites, and with unfilled 3d orbitals, which saturate the cracking products. Transition metals such as nickel (Ni) and molybdenum (Mo) have been widely utilized in previous studies as impregnated metals in catalysts [19–22].

Research conducted by Nadia et al. [15] demonstrated that silica catalysts synthesized from TEOS and impregnated with Ni and Mo enhance acidity, activity, and selectivity for biogasoline production. Similarly, Sowe et al. [21] used a Mo-Ni/HZ catalyst to convert palm oil mill effluent into vegetable-based fuel. Hydrocracking reactions facilitated by Mo-Ni/HZ catalysts have shown significant potential in producing biofuels as substitutes for petroleum-derived fuels. Our previous study [22] reported that the combination of nickel-molybdenum effectively enhanced the performance of sulfated silica, achieving a biogasoline yield of 55.37% from used palm cooking oil through catalytic hydrocracking. Accordingly, this study focuses on synthesizing silica catalysts from rice husk ash and impregnating them with Ni and Mo metals to create $NiMo/SiO_2$ catalysts for the hydrocracking of used palm cooking oil into liquid biofuels. This research aims to contribute novel insights and innovative solutions for advancing biofuel production.

2. Materials and Methods

2.1. Materials

The materials used in this study included locally sourced rice husks from Yogyakarta and used palm cooking oil collected from household waste. Sodium hydroxide (NaOH), 37% hydrochloric acid (HCl), ammonium heptamolybdate tetrahydrate ($(NH_4)_6Mo_7O_{24}\cdot 4H_2O$), nickel(II) nitrate hexahydrate ($Ni(NO_3)_2\cdot 6H_2O$), ammonia (NH_3) were purchased from Merck Company Ltd. Nitrogen gas (N_2), hydrogen gas (H_2), and deionized water were supplied by PT. Surya Indotim Imex.

2.2. Synthesis of silica (SiO_2) from rice husk ash

Rice husks are first washed with deionized water, dried under sunlight, and then burned in a furnace with air circulation at 700 °C for 3 h until they turn into ash. The resulting rice husk ash is soaked in a 1 M HCl solution and stirred for 30 min. Afterward, the mixture is filtered and rinsed with deionized water, and the ash is dried in an oven at 100 °C for 1 h. Next, 10 g of the dried ash are mixed with 60 mL of 1 M NaOH solution and stirred at 80 °C for 1 h. The mixture is then filtered and washed with 100 mL of hot distilled water. The filtrate, a sodium silicate solution, is subjected to an initial pH measurement. It is then titrated with 1 M HCl while stirring until the pH reaches 7, causing the solution to condense and form a gel. This gel is dried in an oven at 100 °C until it converts into a powder. Finally, the silica powder is ground and sieved through a 200-mesh sieve.

2.3. Dual metal nickel-molybdenum impregnation on silica

The impregnation of Ni and Mo metals onto silica catalysts was carried out via co-impregnation. The process begins by dissolving ammonium heptamolybdate tetrahydrate $(NH_4)_6Mo_7O_{24}\cdot 4H_2O$ and nickel(II) nitrate hexahydrate $Ni(NO_3)_2\cdot 6H_2O$ in deionized water at varying concentrations of total Ni and Mo metals (1%, 2%, and 3% by weight) relative to the weight of silica. For example, a 1% NiMo catalyst corresponds to 0.5% (w/w) Ni-to-silica and 0.5% Mo-to-silica. The prepared solution is then mixed with 3 g of the previously synthesized silica (SiO_2) and refluxed at 90 °C for 4 h.

After refluxing, the mixture is dried in an oven at 100 °C for 3 h and subsequently calcined under a flow of nitrogen gas (20 mL/min) at 500 °C for 3 h. Following calcination, the sample undergoes reduction using hydrogen gas (20 mL/min) at 400 °C for 3 h, resulting in the formation of $NiMo/SiO_2$ catalysts.

2.4. Catalysts characterization

The functional groups in all catalyst materials were characterized using a Fourier Transform Infrared spectrometer (FTIR, Nicolet Avatar 360 IR). The presence of Ni and Mo after impregnation was analyzed using an X-ray Diffractometer (XRD, Shimadzu XRD-6000). The textural properties of the catalyst materials were determined with a Surface Area Analyzer (SAA, Quantachrome NovaWin 1200e, version 2.2).

The surface morphology and elemental composition of the catalysts were examined using a Scanning Electron Microscope coupled with an Energy Dispersive X-ray Spectrometer (SEM-EDX, JEOL JSM-6510).

2.5. Acidity measurement of the catalysts

The acidity test was performed using the gravimetric method with ammonia as the adsorbate. The procedure began by placing an empty porcelain crucible in an oven at 100 ºC for 2 h, after which its weight was recorded as W1. As much as 0.05 g sample of each catalyst (SiO_2, NiMo/SiO_2 1%, 2%, and 3% by weight) was placed into the crucible, oven-dried at 100 ºC for 2 h, and then weighed as W2. The crucible containing the catalyst was then transferred to a sealed desiccator, where ammonia vapors were introduced and left to adsorb for 24 h. After the adsorption period, the sample was weighed again as W3. The total acidity of the catalysts was calculated using Eq. (1).

$$\text{Total acidity (mmol/g)} = \frac{(W3-W2)}{(W2-W1) \times MW\ NH_3} \times 1000\ \frac{\text{mmol}}{\text{g}} \quad (1)$$

2.6. Catalytic performance test in the hydrocracking of used palm cooking oil

The thermal hydrocracking of used palm cooking oil to determine the optimum temperature was conducted using 10 g of feed without a catalyst. The process was carried out in a semi-batch microreactor with a hydrogen gas flow rate of 20 mL/min for 60 min at temperature variations of 400, 425, and 450 °C. The temperature that yielded the highest amount of liquid product was identified as the optimum temperature and was used in the subsequent catalytic hydrocracking experiments.

Catalytic hydrocracking was performed at the optimum temperature with a hydrogen gas flow rate of 20 mL/min for 60 min. A catalyst-to-feed ratio of 1:100 (w/w) was used with the following catalysts: SiO_2, NiMo/SiO_2 1, NiMo/SiO_2 2, and NiMo/SiO_2 3. The catalyst that produced the highest biofuel yield was further tested with catalyst-to-feed ratio variations of 1:100, 1:200, and 1:300 (w/w) under the same temperature, hydrogen gas flow rate, and reaction time. The percentages of residue (R), liquid product (LP), and gas product (GP) were calculated using Eq. (2)–(4).

$$R = \frac{W_{\text{container final (g)}} - W_{\text{container initial (g)}}}{W_{\text{feed (g)}}} \times 100\% \quad (2)$$

$$LP = \frac{W_{LP}}{W_{\text{feed}}} \times 100\% \quad (3)$$

$$GP = (100 - R - LP)\% \quad (4)$$

The collected liquid product was then analyzed by Gas Chromatography-Mass Spectrometer (GC-MS, QP2010S Shimadzu). The yield of gasoline (G), diesel (D), non-hydrocarbon (NH), and total biofuel (BF) fractions was determined using Eqs. (5)–(8).

$$G = \frac{\text{GC area of } C_5-C_{12}}{\text{Total GC area}} \times LP\ (\%) \quad (5)$$

$$D = \frac{\text{GC area of } >C_{12}}{\text{Total GC area}} \times LP\ (\%) \quad (6)$$

$$NH = \frac{\text{GC area of non-hydrocarbon}}{\text{Total GC area}} \times LP\ (\%) \quad (7)$$

$$BF = (G + D)\% \quad (8)$$

3. Results and Discussion

3.1. Analysis of functional groups and acidity

The FTIR spectra of silica extracted from rice husk ash and silica impregnated with nickel-molybdenum at various concentrations are shown in Fig. 1. A broad peak in the range of 3300–3600 cm^{-1} corresponds to the stretching vibration of −OH groups from Si−OH bonds, while the peak around 1600 cm^{-1} represents the bending vibration of −OH groups from Si−OH bonds. Peaks at approximately 800 cm^{-1} and 1100 cm^{-1} are attributed to the symmetric and asymmetric stretching vibrations of Si–O–Si bonds, respectively [23]. Additionally, a vibrational peak in the range of 455–480 cm^{-1} indicates the bending vibration of Si–O–Si bonds. The absence of new peaks in the FTIR spectra suggests that Ni and Mo metals were not detected, indicating that the metals do not significantly alter the absorption peaks of silica. This result implies that the interaction between Ni and Mo metals and silica is primarily electrostatic, due to the significant difference in electronegativity between the metals and the silica functional groups or atoms [24].

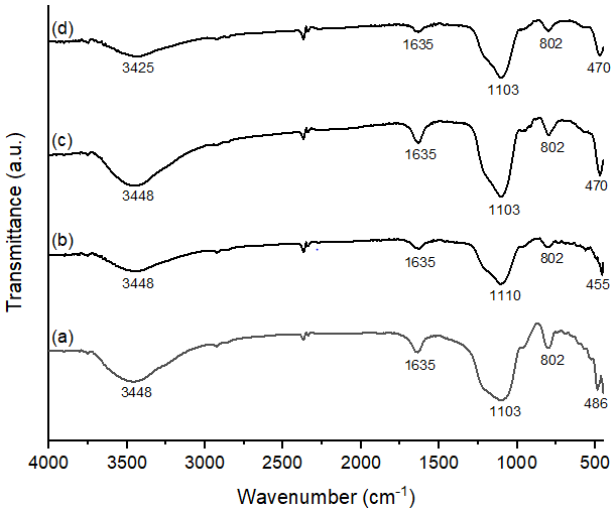

Fig. 1. FTIR spectra of (a) SiO_2, (b) NiMo/SiO_2 1, (c) NiMo/SiO_2 2, and (d) NiMo/SiO_2 3

Various concentrations of nickel and molybdenum were investigated to determine the optimum concentration of NiMo dispersed on silica catalysts. Determining the optimal concentration is essential because excessive metal loading can cause uneven distribution on the silica surface and the formation of aggregates, leading to decreased catalytic activity. Conversely, insufficient metal loading results in a scarcity of acidic sites on the catalyst, limiting its catalytic activity in the hydrocracking reaction [10,22].

The acidity properties of the catalyst play a crucial role in

the cracking process. According to Wijaya et al. [10], the incorporation of transition metals promotes the formation of Lewis acid sites on the catalyst, which are involved in hydrogenation processes and the generation of reactive carbenium species. In this study, ammonia was chosen as the adsorbate for acidity testing due to its smaller molecular size compared to pyridine, enabling interactions not only on the surface but also within the catalyst pores [25]. Thus, ammonia as a probe molecule provides a comprehensive measure of the total acidity of the catalyst. Table 1 presents the catalyst acidity, where the amount of adsorbed ammonia corresponds to the total acidity of the catalysts.

Table 1. Total acidity of the catalysts obtained by NH_3 gravimetric method

Catalyst	Total acidity (mmol/g)
SiO_2	1.88
NiMo/SiO_2 1	3.29
NiMo/SiO_2 2	4.34
NiMo/SiO_2 3	3.99

It was observed that NiMo-impregnated catalysts exhibit higher acidity compared to silica without metal impregnation. This finding is consistent with the work of Nadia and co-workers [15], who reported that the impregnation of transition metals (Ni and Mo) increases the number of acidic sites, thereby enhancing catalyst acidity. Additionally, an increase in acidity from the NiMo/SiO_2 1 catalyst to the NiMo/SiO_2 2 catalyst suggests that a higher concentration of NiMo enhances the acidity of the silica catalyst. However, a decrease in acidity was observed in the NiMo/SiO_2 3 catalyst. According to Wijaya and co-workers [3], this decline may be due to uneven metal distribution on the silica surface, leading to metal aggregation and reducing the adsorption of ammonia.

3.2. X-ray diffractogram analysis

The XRD patterns of SiO_2, NiMo/SiO_2 1, NiMo/SiO_2 2, and NiMo/SiO_2 3 are shown in Fig. 2. The diffraction peak at $2\theta \approx 22°$ confirms the amorphous nature of silica [23]. However, crystalline peaks at 2θ values of 27.2°, 28.3°, 31.6°, 40.4°, and 45.3° indicate the presence of NaCl crystals, as identified by ICDD 00-005-0628. The formation of NaCl crystals may be attributed to incomplete washing of raw materials and gels, leading to the reaction of residual Cl^- ions with Na^+ ions during the extraction process. Notably, the XRD patterns of NiMo/SiO_2 catalysts do not exhibit significant changes, suggesting that variations in metal concentration do not alter the catalyst phase. This outcome can be attributed to the low concentrations of nickel and molybdenum dispersed on the silica catalyst, resulting in weak-intensity absorption peaks.

3.3. Surface and pore characteristics study

The textural properties of the catalyst materials, such as specific surface area, total pore volume, and average pore diameter, play a crucial role in determining catalyst activity during the hydrocracking process. The specific surface area was determined using the Brunauer–Emmett–Teller (BET) equation, while pore volume and diameter were calculated using the Barrett–Joyner–Halenda (BJH) method. Table 2 presents the textural properties of SiO_2, NiMo/SiO_2 1, NiMo/SiO_2 2, and NiMo/SiO_2 3 catalysts. It is clear that the impregnation of Ni and Mo increases the specific surface area of the silica catalysts, with the highest specific surface area observed for the NiMo/SiO_2 2 catalyst. This enhancement is attributed to the loading of metal ions, which increases the catalyst's surface area [26].

Furthermore, increasing the concentration of impregnated metals enhances the number of active sites, thereby improving the catalyst's adsorption capacity for N_2 gas [27]. However, the NiMo/SiO_2 3 catalyst exhibits a decrease in specific surface area. Nadia and colleagues [15] suggest that this reduction is due to uneven metal distribution within the silica pores, leading to metal accumulation and pore blockage. In addition to the specific surface area, the total pore volume of the catalysts increases, with the NiMo/SiO_2 2 catalyst showing the largest total pore volume. Pratika et al. [9] note that calcination time significantly impacts pore volume, with longer calcination times resulting in increased pore volume. The pore diameters of all catalysts fall within the mesoporous range of 2–50 nm [28]. The average pore diameters of the NiMo/SiO_2 catalysts are smaller compared to silica, likely due to pore closure caused by the dual metal loading.

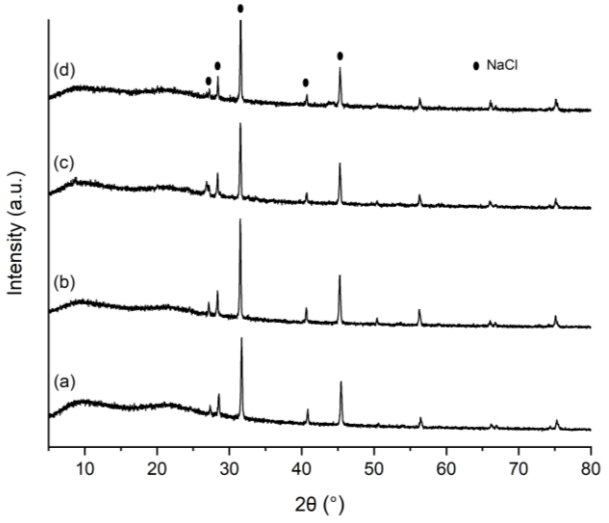

Fig. 2. XRD patterns of (a) SiO_2, (b) NiMo/SiO_2 1, (c) NiMo/SiO_2 2, and (d) NiMo/SiO_2 3

Table 2. Textural properties of the catalysts obtained by SAA

Catalyst	Specific surface area (m_2/g)	Total pore volume (cm^3/g)	Average pore diameter (nm)
SiO_2	124.26	0.58	6.31
NiMo/SiO_2 1	174.42	0.71	5.88
NiMo/SiO_2 2	205.51	0.88	5.91
NiMo/SiO_2 3	123.43	0.53	6.23

The nitrogen gas adsorption-desorption isotherm curves, shown in Fig. 3, were used to analyze the porosity of the catalyst materials. According to Blanco et al. [29], the isotherm curves for all four catalysts correspond to type IV, as classified by the IUPAC, confirming that the catalysts are mesoporous

with pore sizes ranging from approximately 2 to 50 nm. The curves also exhibit hysteresis patterns, which provide information about the pore structure of the materials. All catalyst curves show an H3-type hysteresis pattern, indicating the presence of plate-like particles and slit-shaped pores with irregular shapes and sizes [30].

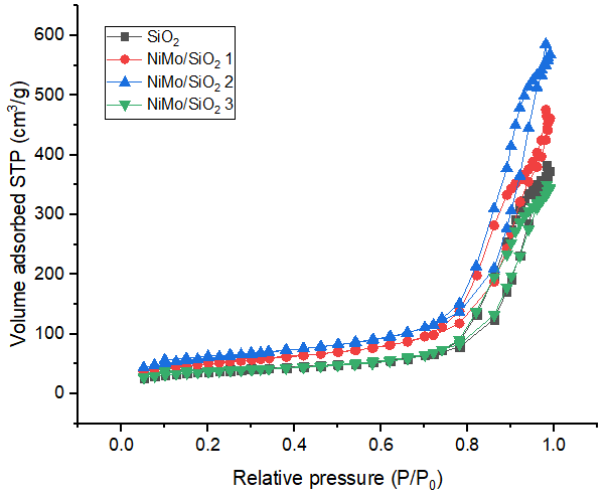

Fig. 3. N_2 adsorption-desorption isotherm curves of the catalysts

Fig. 4 shows the pore diameter distribution curves for all catalyst materials. The pore sizes range from 1 to 14 nm, confirming that all four catalyst materials possess micro- to mesoporous structures, with the majority falling within the mesoporous range. The incorporation of nickel-molybdenum into silica enhances the frequency of both micropores and mesopores, which aligns with the total pore volume data presented in Table 2.

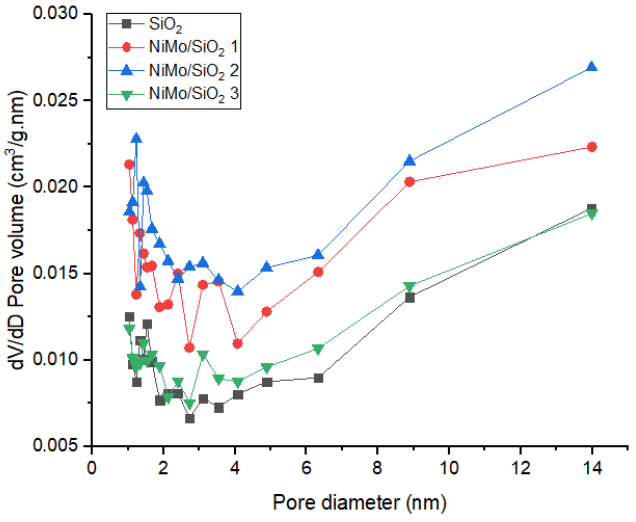

Fig. 4. Pore diameter distribution curves of the catalysts

3.4. Morphological and surface elemental analysis

Fig. 5 presents the surface morphology of the catalysts at a magnification of 3000×. The SEM image of SiO_2 shows a relatively smooth surface compared to the other catalysts. In contrast, the SEM images of the NiMo/SiO_2 1, NiMo/SiO_2 2, and NiMo/SiO_2 3 catalysts display irregularly shaped particles of varying sizes on the catalyst surface. These differences in surface morphology between the SiO_2 and NiMo/SiO_2 catalysts indicate structural changes in the silica after impregnation with Ni and Mo metals.

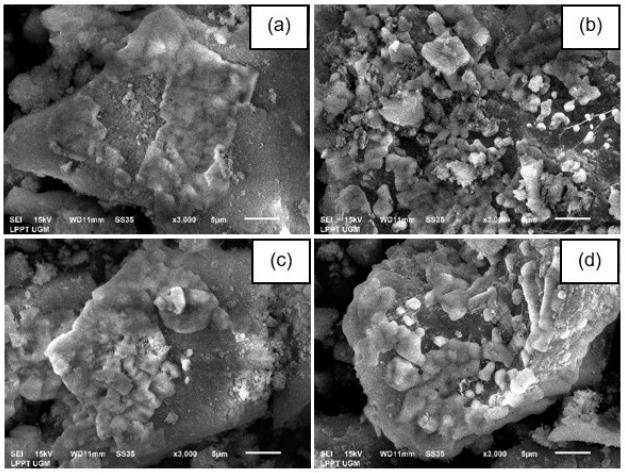

Fig. 5. SEM micrographs of (a) SiO_2, (b) NiMo/SiO_2 1, (c) NiMo/SiO_2 2, and (d) NiMo/SiO_2 3 at 3,000× magnification

Table 3. Elemental composition of the catalysts obtained by EDX

Catalyst	Elemental composition (wt%)						
	C	Si	O	Na	Cl	Ni	Mo
SiO_2	11.86	17.62	31.67	17.37	21.48	Nd	Nd
NiMo/SiO_2 1	14.51	14.40	22.56	20.76	27.30	0.47	Nd
NiMo/SiO_2 2	13.91	19.14	26.49	16.09	22.53	1.16	0.68
NiMo/SiO_2 3	13.65	25.30	34.44	12.44	11.06	1.82	1.29

Nd = not detected

EDX data were obtained to determine the elemental compositions of the catalysts, as shown in Table 3. The data reveal that the concentrations of Ni and Mo in the NiMo/SiO_2 1, NiMo/SiO_2 2, and NiMo/SiO_2 3 catalysts are significantly lower than the intended impregnation concentrations. This discrepancy can likely be attributed to the uneven distribution of Ni and Mo metals on the catalyst surface [10].

3.5. Hydrocracking of used palm cooking oil over the catalysts

The thermal hydrocracking process was conducted at varying temperatures to determine the optimal conditions for converting used palm cooking oil into biofuel and maximizing the liquid product yield. Hydrocracking was performed without a catalyst at temperatures of 400 °C, 425 °C, and 450 °C. Based on Fig. 6, the highest percentage of liquid product (18.7% of the feed mass) was obtained at 450 °C, indicating that this temperature optimizes vaporization of the feed.

Subsequently, the performance of the synthesized catalysts was evaluated for the conversion of used palm cooking oil into biofuels at 450 °C. The hydrocracking products included liquid and gas fractions, along with non-vaporizable residue remaining in the reactor. The percentages of hydrocracking products for various catalysts are summarized in Table 4.

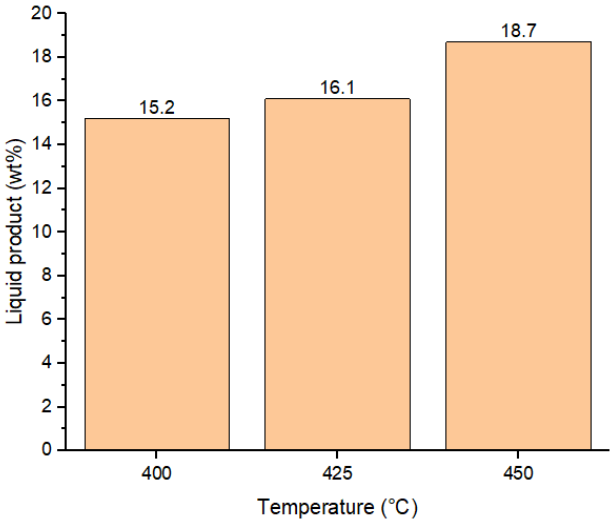

Fig. 6. The amount of liquid product obtained at various thermal hydrocracking temperatures

Table 4. Product conversion of hydrocracking using various catalysts

Catalyst	Conversion (wt%)		
	Residue	Liquid product	Gas product
Thermal 450 °C	30.0	18.7	51.3
SiO_2	40.0	19.5	40.5
NiMo/SiO_2 1	30.0	22.4	47.6
NiMo/SiO_2 2	30.0	23.3	46.7
NiMo/SiO_2 3	30.0	20.9	49.1

As seen in Table 4, thermal hydrocracking produces a higher proportion of gaseous products compared to catalytic hydrocracking. This result aligns with the findings of previous studies, where the radical reactions induced by high temperatures in thermal hydrocracking favor the breakdown of long-chain hydrocarbons into gaseous short-chain fractions [31]. However, the introduction of dual metal nickel-molybdenum onto SiO_2 increased the yield of the liquid product, with the highest percentage observed using the NiMo/SiO_2 2 catalyst. This trend correlates with the total acidity data in Table 1, which indicates that the NiMo/SiO_2 2 catalyst has the highest total acidity. High catalyst acidity promotes the formation of carbenium ions, which serve as initiators in the hydrocracking reaction, thereby enhancing catalytic activity and liquid product yield [32].

The selectivity of hydrocarbon fractions in the resulting liquid product was determined through GC-MS analysis. The gasoline fraction comprises hydrocarbons in the C_5–C_{12} range, while the diesel fraction includes hydrocarbons with a carbon number greater than C_{12}. The total yield of the gasoline and diesel fractions represents the biofuel yield. Additionally, the liquid product contains non-hydrocarbon compounds such as residual fatty acids, aldehydes, ketones, and alcohols, which are by-products of the hydrocracking reaction. The yields of the hydrocarbon fractions are summarized in Table 5.

As shown in Table 5, thermal hydrocracking produces the highest percentage of non-hydrocarbon fractions. This result suggests that, in the absence of a catalyst, the hydrodeoxygenation reaction (oxygen atom removal) does not proceed efficiently alongside hydrocracking. With the use of catalysts, the non-hydrocarbon fraction decreases significantly, with the NiMo/SiO_2 2 catalyst yielding the lowest percentage of non-hydrocarbon by-products.

Table 5. Liquid product yield of hydrocracking using various catalysts

Catalyst	Yield (wt%)			
	Gasoline	Diesel	Biofuel	Non-hydrocarbon
Thermal 450 °C	11.40	4.93	16.33	2.38
SiO_2	10.81	5.12	15.93	1.96
NiMo/SiO_2 1	13.14	5.85	18.99	1.74
NiMo/SiO_2 2	14.20	6.14	20.34	0.56
NiMo/SiO_2 3	12.37	6.28	18.65	0.87

Catalytic hydrocracking using the SiO_2 catalyst produced a lower yield of biofuel fractions compared to thermal hydrocracking. This may be due to the non-directed nature of the hydrocracking reaction without a catalyst, resulting in the formation of non-selective hydrocarbon fractions. The NiMo/SiO_2 2 catalyst, however, achieved the highest biofuel fraction yield (20.34%), consisting of 14.20% gasoline fraction and 6.14% diesel fraction. These results demonstrate that higher catalyst acidity enhances the selectivity of feed conversion into biofuel fractions by increasing the availability of active sites, which are critical for the hydrocracking process [28].

Table 6. Product conversion of hydrocracking using the NiMo/SiO_2 2 catalyst at various catalyst-to-feed ratios

Catalyst-to-feed ratio (w/w)	Conversion (wt%)		
	Residue	Liquid product	Gas product
1:100	30.0	23.3	46.7
1:200	30.0	20.7	49.3
1:300	30.0	19.2	50.8

To determine the optimal catalyst-to-feed weight ratio for maximizing biofuel production, hydrocracking experiments were conducted at catalyst-to-feed ratios of 1:100, 2:100, and 3:100 (w/w) using the NiMo/SiO_2 2 catalyst at the optimum temperature. The results, summarized in Table 6, indicate that the highest percentage of liquid product was achieved at a catalyst-to-feed weight ratio of 1:100. As shown in Table 6, increasing the feed amount relative to the catalyst resulted in a decline in liquid product yield, with the lowest yield (19.2%) obtained at a catalyst-to-feed ratio of 1:300. This decrease may be due to the excessive adsorption of feed molecules, leading to active site blockage and reduced catalytic efficiency [33]. Higher feed amounts may also intensify the hydrocracking reaction, favoring the formation of gaseous hydrocarbon fractions [31].

Table 7 presents the yields of biofuel fractions obtained

from catalytic hydrocracking at different catalyst-to-feed weight ratios. The highest gasoline fraction yield (14.20%) was achieved at a catalyst-to-feed ratio of 1:100. In all weight ratio variations, the gasoline fraction yield consistently exceeded the yields of diesel and non-hydrocarbon fractions. According to Agharadatu et al. [34], excessive hydrocarbon reactions at higher feed amounts can lead to increased coke deposition, which reduces the yield of biofuel fractions.

Table 7. Liquid product yield of hydrocracking using the NiMo/SiO_2 2 catalyst at various catalyst-to-feed ratios

Catalyst-to-feed ratio (w/w)	Yield (wt%)			
	Gasoline	Diesel	Biofuel	Non-hydrocarbon
1:100	14.20	6.14	20.34	0.56
1:200	10.78	9.35	20.13	0.24
1:300	10.62	6.58	17.20	0.00

The present study has successfully revealed the significant potential of rice husk ash as a source of biogenic silica for nickel-molybdenum bimetal support, thereby enhancing the sustainability of the biofuel industry. The utilization of used palm cooking oil as feedstock in biofuel production is another significant innovation in waste utilization and supporting the circular economy. However, it is important to note that further research is necessary to conduct a feasibility test on our biofuel production for industrial upscale in the future.

4. Conclusion

The synthesis of NiMo/SiO_2 catalysts with varying NiMo bimetal concentrations (1%, 2%, and 3% wt) was successfully achieved using rice husk ash as a silica source. The impregnation of nickel-molybdenum significantly altered the physicochemical properties of the untreated silica. Among the variations, the NiMo/SiO_2 catalyst with 2% NiMo concentration (NiMo/SiO_2 2) demonstrated optimal performance in terms of total acidity, specific surface area, and total pore volume. Hydrocracking at an optimal temperature of 450 °C, with a hydrogen gas flow rate of 20 mL/min for 1 h, and a catalyst-to-feed ratio of 1% yielded the highest liquid product and biofuel fraction at 23.3% and 20.34%, respectively. Future research should focus on testing the reusability of the catalyst and evaluating the physical properties of the biogasoline produced. These findings present an innovative approach that can potentially be applied in industrial biofuel production using environmentally friendly catalysts derived from abundant natural resources.

Acknowledgements

The authors would like to express their gratitude to the Indonesian Collaboration Research Program-10 (PTNBH), Universitas Gadjah Mada, Universitas Brawijaya, Universitas Diponegoro, and Universitas Sebelas Maret for their financial support in this research under contract number 2051/UN1.P.III/DIT-LIT/LT/2019 for the Fiscal Year 2019.

References

1. B. Sharma, A. Shrestha, *Petroleum dependence in developing countries with an emphasis on Nepal and potential keys*, Energy Strategy Reviews 45 (2023) 101053.
2. J. Blanco-Cejas, S. Martín, M. Linares, J. Iglesias, J. Moreno, *Life cycle assessment applied to bio-based platform molecules: Critical review of methodological practices*, J. Clean. Prod. 414 (2023) 137513.
3. K. Wijaya, M.A. Kurniawan, W.D. Saputri, W. Trisunaryanti, M. Mirzan, P.L. Hariani, A.D. Tikoalu, *Synthesis of nickel catalyst supported on ZrO_2/SO_4 pillared bentonite and its application for convertision of coconut oil into gasoline via hydrocracking process*, J. Environ. Chem. Eng. 9 (2021) 105399.
4. S. Brahma, B. Nath, B. Basumatary, B. Das, P. Saikia, K. Patir, S. Basumatary, *Biodiesel production from mixed oils: a sustainable approach towards industrial biofuel production*, Chem. Eng. J. Adv. 10 (2022) 100284.
5. Z. Pei, L. Luo, *Biofuels from renewable sources, a potential option for biodiesel production*, Bioengineering (Basel) 10 (2023) 29.
6. A.M. Eremeeva, K. Natalia, Kondrasheva, A.F. Khasanov, I..L. Oleynik, *Environmentally friendly diesel fuel obtained from vegetable raw materials and hydrocarbon crude*, Energies 16 (2023) 2121.
7. S.S. Wirawan, D. Maharani, Solikhah, H. Setiapraja, A. Sugiyono, *Biodiesel implementation in Indonesia: Experiences and future perspectives*, Renew. Sustain. Enegy Rev. 189 (2024) 113911.
8. K. Wijaya, A. Syoufian, S.D. Ariantika, *Hydrocracking of used cooking oil into biofuel catalyzed by nickel-bentonite*, Asian J. Chem. 26 (2014) 3785–3789.
9. R.A. Pratika, K. Wijaya, W. Trisunaryanti, *Hydrothermal Treatment of SO_4/TiO_2 and TiO_2/CaO as heterogeneous catalysts for the conversion of jatropha oil into biodiesel*, J. Environ. Chem. Eng. 9 (2021) 106547.
10. K. Wijaya, A. Nadia, A. Dinana, A.F. Pratiwi, A.D. Tikoalu, A.C. Wibowo, *Catalytic hydrocracking of fresh and waste frying oil over Ni- and Mo- based catalyst supported n sulfated silica for biogasoline production*, Catalysts 11 (2021) 1150.
11. I. Istadi, T. Riyanto, E. Khofiyanda, L. Buchori, D.D. Anggoro, I. Sumantri, B.H.S. Putro, A.S. Firnanda, *Low-oxygenated biofuels production from palm oil through hydrocracking process using the enhanced spent RFCC catalysts*. Bioresour. Technol. Rep. 14 (2021) 100677.
12. K. Wijaya, R.A. Pratika, W. Trisunaryanti, A.D. Tikoalu, *Modification of TiO_2 as SO_4/TiO_2 acid and CaO/TiO_2 base catalysts and their applications in conversion of waste frying oil (WFO) into biodiesel*. In: Ikhmayies, S.J. (eds) Advances in Catalysts Research. Advances in Material Research and Technology (2024) 377–414.
13. M.U.H. Suzihaque, H. Alwi, U.K. Ibrahim, S. Abdullah, N. Haron, *Biodiesel production from waste cooking oil: a brief review*, Mater. Today: Proc. 63 (2022) S490–S495.
14. L. Xin-Fang, S. Jumat, M.M. Rais, J. Kamsiah, *Effect of repeatedly heated palm olein on blood pressure—regulating enzymes activity and lipid peroxidation in rats*, Malays. J. Med. Sci. 19 (2012) 20–29.
15. A. Nadia, K. Wijaya, I.I. Falah, S. Sudiono, A. Budiman, *Self-regenation of monodisperse hierarchical porous NiMo/Silica catalyst induced by $NaHCO_3$ for biofuel production*, Waste Biomass Valor. 13 (2022) 2335-2347.
16. P.U. Nzereogu, A.D. Omah, F.I. Ezema, E.I. Iwuoha, A.C. Nwanya, *Silica extraction from rice husk: comprehensive review and applications*, Hybrid Advances 4 (2023) 100111.
17. R. Mohadi, N.R. Palapa, T. Taher, P.M.S.B.N. Siregar, Normah, N. Juleanti, A. Wijaya, A. Lesbani, *Removal of Cr(VI) from aqueous solution*

by biochar derived from rice husk, Commun. Sci. Tech. 6 (2021) 11–17.

18. A. Aneu, R.A. Pratika, Hasanudin, S. Gea, K. Wijaya, W.-C. Oh, *Silica-based catalysts for biodiesel production: a brief review*, Silicon 15 (2023) 5037–5047.
19. G.D. Alisha, W. Trisunaryanti, A. Syoufian, *Mesoporous Silica from Parangtritis Beach Sand Templated by CTAB as a Support of Mo Metal as a Catalyst for Hydrocracking of Waste Palm Cooking Oil into Biofuel*, Waste Biomass Valor 13 (2022) 1311–1321.
20. W. Trisunaryanti, Triyono, K. Wijaya, I. Kartini, S. Purwono, Rodiansono, A. Mara, A. Budiansyah, *Preparation of Mo-impregnated mordenite catalysts for the conversion of refined kernel palm oil into bioavtur*, Commun. Sci. Tech. 8 (2023) 226–234.
21. M.S. Sowe, A.R. Lestari, E. Novitasari, M. Masruri, S.M. Ulfa, *The production of green diesel rich pentadecane (C15) from catalytic hydrodeoxygenation of waste cooking il using Ni/Al_2O_3-ZrO_2 and Ni/SiO_2-ZrO_2*, Bull. Chem. React. Eng. 17 (2022) 135–145.
22. K. Wijaya, S. Ramadhani, A.J. Saviola, N. Prasetyo, S. Gea, L. Hauli, A.K. Amin, W.D. Saputri, D.A. Saputra, N. Darsono, *Efficient conversion of used palm cooking oil into biogasoline over hydrothermally prepared sulfated mesoporous silica loaded with NiMo catalyst*, Results Eng. 24 (2024) 103185.
23. R.A. Pratika, K. Wijaya, M. Utami, S. Mulijani, A. Patah, S. Alarifi, R.R. Mani, K.K. Yadav, B. Ravindran, W.J. Chung, S.W. Chang, G.M. Ramanujam, *The potency of hydrothermally prepared sulfated silica (SO4/SiO2) as a heterogeneous acid catalyst for ethanol dehydration into diethyl ether*, Chemosphere 341 (2023) 139822.
24. T.K.K. Do, C.T. Nguyen, N.M. Huynh, *Effect of temperature on the ability to synthesize SiC from rice husk*, Mater. Res. Express 11 (2024) 055510.
25. C. Morterra, G. Cerrato, F. Pinna, G. Meligrana, *Limits in the use of pyridine adsorption, as an analyticaal tool to test the surface acidity of oxidic system. The case of sulfated ziconia catalysts*, Topics in Catalysis 15 (2021) 53–61.
26. A.S. Sadeek, E.A. Mohammed, M. Shaban, M.T.H. Kana, N.A. Negm, *Synthesis, characterization and catalytic performances of activated carbon-doped transition metals during biofuel production from waste cooking oils*, J. Mol. Liq. 306 (2020) 112749.
27. R. Rasyid, R. Malik, H.S. Kusuma, A. Roesyadi, M. Mahfud, *Triglycerides hydrocracking reaction of nyamplung oil with non- sulfided $CoMo/\gamma$-Al_2O_3 catalysts*, Bull. Chem. React. Eng. 13 (2018) 196–203.
28. K. Wijaya, T.S. Ningrum, A.J. Saviola, N. Prasetyo, Z.L. Ardelia, R.A. Fitria, S. Gea, L. Hauli, A.K. Amin, W.D. Saputri, A. Setiawan, W.-C. Oh, *Development of chromium-impregnated sulfated silica as a mesoporous catalyst in the production of biogasoline from used cooking oil via a hydrocracking process*, React. Kinet. Mech. Catal. 137 (2024) 971–989.
29. P.H. Blanco, C. Wu, J.A. Onwudili, P.T. Williams, *Characterization and evaluation of Ni/SiO_2 catalysts for hydrogen production and tar production from catalytic steam pyrolisis-reforming of refuse derived fuel*, App. Catal. B: Environ. 134 (2013) 238–250.
30. A.M. Rabie, E.A. Mohammed, N.A. Negm, *Feasibility of modified bentonite as acidic heterogeneous catalyst in low temperature catalytic cracking process of biofuel production from nonedible vegetable oils*, J. Mol. Liq. 254 (2018) 260–266.
31. M. Utami, W. Trisunaryanti, K. Shida, M. Tsushida, H. Kawakita, K. Ohto, K. Wijaya, M. Tominaga, *Hydrothermal preparation of a platinum-loaded sulphated nanozirconia catalyst for the effective conversion of waste low density polyethylene into*, RSC Adv. 9 (2019) 41392–41401.
32. A.J. Saviola, K. Wijaya, A. Syoufian, W.D. Saputri, D.A. Saputra, I.T.A. Aziz, W.-C. Oh, *Hydroconversion of used palm cooking oil into bio-jet fuel over phosphoric acid-modified nano-zirconia catalyst*, Case Studies in Environ. Eng. 9 (2024) 100653.
33. M.D. Argyle, C.H. Bartholomew, *Heterogeneous catalyst deactivation and regeneration: a review*, Catalysts 5 (2015) 145–269.
34. R.H. Agharadatu, K. Wijaya, Wangsa Prastyo, L. Hauli, W.-C. Oh, *Application of mesoporous NiMo/silica ($NiMo/SiO_2$) as a catalyst in the hydrocracking of used cooking oil into jet fuel*, Silicon 16 (2024) 331–343.